



## Electric charge of atmospheric nanoparticles and its potential implications with human health



Pablo Fdez-Arroyabe<sup>a,\*</sup>, Ciro Salcines<sup>b</sup>, Pavlos Kassomenos<sup>c</sup>, Ana Santurtún<sup>d</sup>, Tuukka Petäjä<sup>e</sup>

<sup>a</sup> University of Cantabria, Department of Geography and Planning, Geobiomet Research Group, Santander, Spain

<sup>b</sup> University of Cantabria, Health and Safety Unit, Infrastructures Service, Santander, Spain

<sup>c</sup> University of Ioannina, Department of Physics, Laboratory of Meteorology, GR-45110 Ioannina, Greece

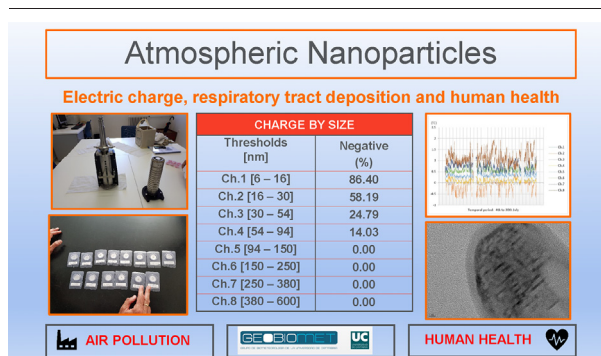
<sup>d</sup> University of Cantabria, Department of Physiology and Pharmacology, Geobiomet Research Group, Santander, Spain

<sup>e</sup> Institute for Atmospheric and Earth System Research (INAR), Physics, Faculty of Science, FI-00014 University of Helsinki, Finland

### HIGHLIGHTS

- ELPI®+ can be used to measure pollution by atmospheric nanoparticles.
- Negative charge is predominant in the smallest nanoparticles in maritime aerosol.
- Electric charge is a key metric to improve the nanoparticles deposition knowledge.

### GRAPHICAL ABSTRACT



### ARTICLE INFO

#### Article history:

Received 7 October 2021

Received in revised form 27 November 2021

Accepted 27 November 2021

Available online 2 December 2021

Editor: Damia Barcelo

#### Keywords:

Air pollution

Aerosols

ELPI®+

Nanoparticle charge

Human health

Deposition model

### ABSTRACT

This research presents a pilot project developed within the framework of the COST Action 15,211 in which atmospheric nanoparticles were measured in July 2018, in a maritime environment in the city of Santander in Northern Spain. ELPI®+ (Electrical Low-Pressure Impactor) was used to measure nanoparticle properties (electric charge, number, size distribution and surface area) from 6 nm to 10,000 nm with 14 size channels. This study focused on the range between 6 and 380 nm. It considered atmospheric nanoparticle electric charge with surface area, deposited and number by size distribution at human respiratory tract regions in a standard person in Santander according to the human respiratory tract model of ICRP 94. An empirical distribution of nanoparticles deposited in the human respiratory tract model and its electric charge is presented for the city of Santander as the main output. Percentages of total and regional deposition in human respiratory tract model were calculated for the Atlantic climate. Nanoparticles have shown an alveolar surface area deposition plateau with a size distribution range between 6 nm to 150 nm. Negative charge of nanoparticles was clearly associated with primary atmospheric nanoparticles being mainly deposited in the alveolar region where a Brownian mechanism of deposition is predominant. We can demonstrate that electric charge may be a key element in explaining Brownian deposition of the smallest particles in the human respiratory tract and that it can be linked to theoretical positive and negative impacts on human health according to several biometeorological studies. To support our analysis, aerosol samples were characterized with transmission electron microscopy and Confocal Raman spectrometer to determinate morphology, size, chemical composition, and structure. The toxicological effects of the samples with the alveolar surface area had a greater deposition, remain to be studied.

\* Corresponding author.

E-mail addresses: [fernandhp@unican.es](mailto:fernandhp@unican.es) (P. Fdez-Arroyabe), [ciroluis.salcines@unican.es](mailto:ciroluis.salcines@unican.es) (C. Salcines), [pkassom@uoi.gr](mailto:pkassom@uoi.gr) (P. Kassomenos), [ana.santurtun@unican.es](mailto:ana.santurtun@unican.es) (A. Santurtún), [tuukka.petaja@helsinki.fi](mailto:tuukka.petaja@helsinki.fi) (T. Petäjä).

## 1. Introduction

Air pollution is a clear threat to human health and the reduction of anthropogenic emission is probably one of the most important challenges in this century to combat negative impacts of air quality, climate change and global warming (e.g. Campbell et al., 2018; Shindell and Smith, 2019; Lappalainen et al., 2021). Atmospheric pollution related health risk is highly dependent on the properties of the pollutant, the level of exposure which determines the received dose, and the individual vulnerability of the living organisms affected by them (Health Organization et al., 2013; Manisalidis et al., 2020; Ghorani-Azam et al., 2016). Atmospheric pollution networks have become essential to measure air quality in cities, where CO<sub>2</sub> levels and pollutants such as ozone, NO<sub>x</sub>, or Particulate Matter (PM) are recorded systematically.

Atmospheric PM is formed by airborne solid and liquid particles, which toxicity can be a key issue in human health-related studies. Particles with a diameter inferior to 2.5 μm are of maximum interest in this area because can translocate in the human body (Rothen-Rutishauser et al., 2008). Considering the source of pollution, the relevance of coarse particles with low density is also high because they can be deposited deep in the lungs, as it happens with fine particles with high density too (Deng et al., 2019). Health effects of soil dust may be as strong as those cause by traffic particles.

Although numerous studies link PM with respiratory and cardiovascular health (Peters et al., 1997; Wichmann et al., 2000), the composition of the particles is decisive on its effects, both due to its harmfulness and its ability to deposition in the respiratory tract (Santurt et al., 2015; Yang et al., 2020; Hamanaka and Mutlu, 2018; Santurtún et al., 2017).

Currently, due to the strict regulations on air quality, in Spanish cities there are hourly measurements of PM<sub>10</sub> and PM<sub>2.5</sub> carried out by the government. Based on these measurements, political decisions to improve air quality and primary prevention strategies are made. However, nanoparticles (PM<sub>0.1</sub>), which are particles of matter that are between 1 and 100 nm (Comission, 2011), cause more pulmonary inflammation and are more retained in the lung than PM<sub>2.5</sub> and are not measured with standard parameters. In 2020, explained that, on the one hand, the misunderstanding of the impact of nanoparticles on human body conditioned public health studies and, on the other hand, the lack of PM<sub>0.1</sub> measurement led to neither taking measures nor improving protocols (Schraufnagel, 2020). The European Commission recommendation on the definition of nanomaterial includes the classification of nanoparticles (3 dimensions between 1 and 100 nm). Nanoparticles are only, the particles with three dimensions in 1–100 nm range, but it is generally accepted to use nanoparticle and nanomaterial equally; this practice is followed in this paper.

PM standard parameter is the mass and number (particles/cm<sup>3</sup>). Those are precise units to estimate toxicology at micrometer size. Nevertheless, the exponential increase of the surface area (micrometer<sup>2</sup>/cm<sup>3</sup>) of nanometer size requires the addition of surface area as a complementary and necessary measuring unit. Nanotoxicology effects of air intake were possible to study with higher accuracy with surface area than mass (Brown et al., 2001; Tran et al., 1998; Donaldson et al., 1998; Donaldson and Tran, 2002; Oberdörster et al., 1992; Oberdörster and Yu, 1990; Tran, 2000).

Meteorological factors play a key role in the formation and transport of aerosols and can move pollutants from places where they originate to multiple geographic locations (Shenfeld, 2011), (Fisher, 2002). Wind speed and direction are essential factors to determine pollutants concentration and dispersion in urban environments (Zhang et al., 2015). Nanosized matter can be affected by the physical characteristics of the circulation weather types and air masses that transport them (Fdez-Arroyabe et al., 2020) and influence their own properties.

Atmospheric nanoparticles are taken into the human respiratory tract (HRT) much more easily than bigger particulate matter (Qiao et al., 2015). The most vulnerable people in this case are children, elderly and those with chronic diseases. Final deposition of nanoparticles in the human respiratory system is not uniform and this complexity (Löndahl et al., 2014) is explained by different models. Human vulnerability to air pollution also depends on air ways structures and breathing conditions

which vary considerably with age. The dose of particle deposition in infants and children is higher than for adults, being particles mainly deposited in the upper airways for infants but in the lower airways for adults (Deng et al., 2018).

From a biometeorological point of view, negative ion environment can affect various cardiovascular, thermoregulatory and mental functions (Krueger and Reed, 1976; Chu et al., 2019; Liu et al., 2021). The existence of negative ions indoors was correlated with low levels of dust in the air that can be connected to the existence of some respiratory diseases too (Maćzyński et al., 1971). It has been demonstrated that an environment of negative ions has positive effects on the wellbeing of people (Inbar et al., 1982; Hawkins, 1981) reducing by 50% the number of headaches indoors and increasing the subjective rating of alertness, atmospheric freshness and personal warmth. ELPI®+ has been used to study aerosol particle number, surface area, mass and size distribution in urban, rural and high-alpine air (Held et al., 2008). However, few studies have focused on electrical charge. Surface chemistry, number, chemical composition, size distribution and structure are relevant characteristics to study the effect of aerosol particles on health (Donaldson et al., 2005; G. Oberdörster et al., 2005a, 2005b; Oberdörster, 2000; Oberdörster et al., 2009).

Deposited surface area of particles in the human respiratory tract has already been measured with electrical low pressure impactors (Lepistö et al., 2020). However, there is a gap in knowledge of the significance of electrical charge of deposited nanomaterials in the human respiratory tract (HRT). The deposition process appears to be explained Brownian mechanisms (Oberdörster et al., 2005a, 2005b). Nevertheless, it is necessary to study in more detail the interaction of charge, surface area and surface structure and how it affects to surface oxidation and biokinetic behavior (Geiser and Kreyling, 2010). Cardiovascular and respiratory harmful effects of nanoparticles have been shown to be connected (Peters et al., 1997; Wichmann et al., 2000).

The work hypothesis is that electric charge is a key metric to improve the deposition knowledge in the HRT due to unique physicochemical characteristics of nanomaterials. In this work we address this by performing measurements of total and regional deposited fraction of atmospheric nanoparticles in the human respiratory tract in a person of Santander considering nanoparticle electrical charge and surface area across size thresholds and characterising samples with TEM and RAMAN electroscopic techniques.

## 2. Materials and methods

### 2.1. Study area

The city of Santander is a medium-size city (173,000 inhabitants), located in the Northern coast of Spain by the Cantabrian Sea, affected by maritime influences and with a moderate climate, (Cfb) according to Köppen-Geiger classification (Kottek et al., 2006).

### 2.2. Instrumentation and data

The pilot project consisted measurements of atmospheric primary nanoparticle, secondary nanoparticle and microparticle data in the city of Santander. An ELPI®+ was lent by Dekati Ltd. to the Geobiomet Research Group at the University of Cantabria within the framework of the European COST Scientific Action 15211, Electronet. The device was installed on the roof of the Faculty of Philosophy and data were taken across from 14 different channels (Dekati, 2018) during the month of July 2018. (4th July 18:00–30th July 23:50). According to Dekati (2018), the operating principle of ELPI®+ is divided into three stages: a) particle charging with a corona charger; b) inertial size classification of particles in a cascade impactor based on to their aerodynamic size; c) electrical detection of particle charge with sensitive electrometers. A performance evaluation showing the stage operating pressures and collection efficiency curves of the ELPI® can be found in Marjamak et al. (2000). The charger performance

of ELPI®+ is 54% higher at 20 nm particle size compared with the previous ELPI® (Järvinen et al., 2014; Järvinen et al., 2017).

The measurement strategy was based on two cycles. In a first cycle an ELPI + device worked with a charger corona for 30 s measuring the properties of surface area, number concentration, volume, mass, and size diameter. In the second cycle of charger corona was turned off for 30 s, and parameters of current and electric charge were also registered every second. This allowed sequential determination of aerosol parameters after exposing them to charge carrying cluster ions and parameters reflecting naturally charged aerosol population.

Properties of particles were registered per second across 14 different channels from 6 nm to 10,000 nm. Samples of particles were collected weekly. In this preliminary study, a subset of 8 channels formed by those included size from 6 to 380 nm was chosen.

The parameters chosen for this study were: number concentration, surface area charge and diameter size. The first was selected due to be a standardized unit with exposed limits. Surface area is strongly connected with nanotoxicity, and electric charge was considered also due to the lack of knowledge of the role it plays in the deposition of particles in the Human Respiratory Tract Model (HRTM).

Electric charge (fC) is a basic measuring unit to cover the 3 different ranges and is an important and unknown property that affects HRT deposition and its toxicology. The Stokes diameter was used to describe the electric charge of particles and the aerodynamic diameter to calculate the deposition with the predictive mathematical model of the human respiratory tract (International Commission on Radiological Protection, 1994).

Each channel range threshold of ELPI®+ includes Di (nm) Stokes diameter and D50% (nm) aerodynamic diameter measurements. The Stokes diameter is more accurate at our nanoparticle size goal (Dekati, 2018), so it was used to take electric charge measurement. However, the HRTM formula works with the aerodynamic diameter, so we took the equivalent unit of each channel number within each channel range threshold.

The D50% or cut-off diameter is the size of particles collected with 50% efficiency on each impactor stage. According to ELPI®+ nominal impactor specifications, the D50% for each channel and their corresponding threshold are 380 [380–600 nm]; 250 [250–380 nm]; 150 [150–250 nm]; 94 [94–150 nm]; 54 [54–94 nm]; 30 [30–54 nm]; 16 [16–30 nm] and 6 [6–16 nm].

### 2.3. Data analysis methodology

Data preprocessing consisted of cleaning the raw data collected by the ELPI + (one data per channel per second). The 10th and 90th percentiles were used to eliminate extreme values from the temporal series. Mean values were integrated at four temporal scales (10 min, 1 h, 6 and 24 h). Some short periods are empty in the data series due the need to stop the device to collect samples.

The ICRP model was selected to estimate regional deposition of nanoparticles in the HRT (ICRP, 1994). This modelling was used to estimate deposition in the three main regions of the respiratory tract: Head Airways (HA), Tracheobronchial (TB) and Alveolar (AL). Predicted total and regional deposition by the ICRP model (Hinds, 1999) was estimated by channel as a function of particle size, for particles from 6 nm to 10,000 nm. Fig. 1 shows the resulting percentages. Lines represent total, deposition fraction (DF) and regional deposition for the different respiratory zones being HA, TB and AL. Dots in lines symbolize aerodynamic diameter (D50%) [ $\mu\text{m}$ ] for each measurement channels selected of ELPI®+ according to HRTM.

Deposition regions in the respiratory tract have been obtained from the HRTM where HA surface of the extra-thoracic region is estimated to be 470  $\text{cm}^2$ ; airway surface of the bronchial and bronchiolar region is equal to 302.6  $\text{cm}^2$  and airway surface of the alveolar-interstitial region is equal to 147.5  $\text{m}^2$  (ICRP, 1994).

Deposition fraction and regional deposition fraction were calculated for Ch. 1 (6 nm) to Ch. 8 (380 nm). Number, size distribution and surface area were obtained from the measurements. Moreover, charge was also indicated for each considered channel. It must be highlighted that charge was measured for each channel not being possible to distribute it into specific respiratory regions.

## 3. Results and discussion

### 3.1. Number concentration

First, it was observed that number ( $\text{pt}/\text{cm}^3$ ) increases with the decrease in of nanoparticle size. Fig. 2 presents the number of nanoparticles registered for channels from Ch. 1 (6 nm) to Ch. 8 (380 nm) by different regions of the respiratory tract.

Number of smallest particles is consistently high in the three respiratory regions for Ch.1 (6 nm) and has a similar regional deposition. At the same

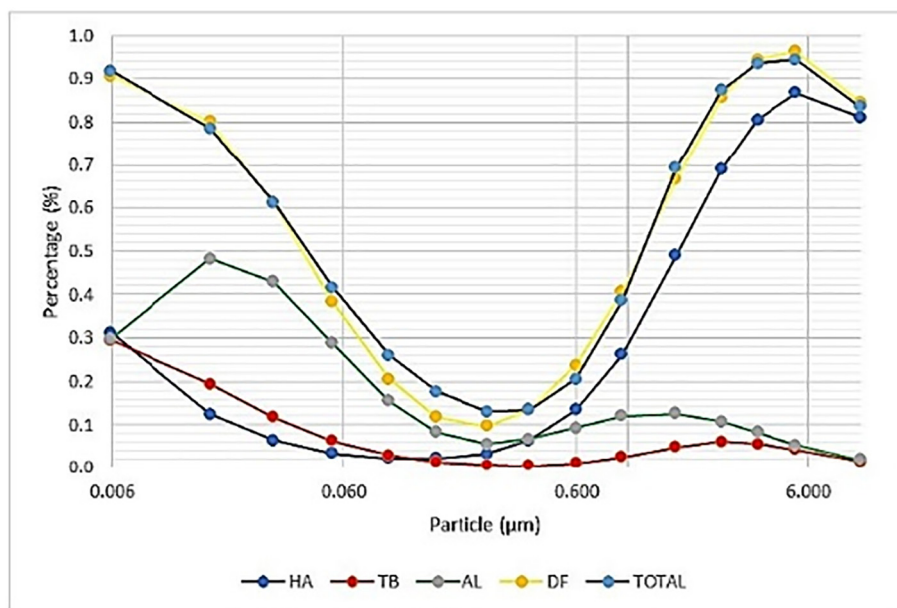


Fig. 1. Total and regional deposition based on the ICRP deposition model (Hinds, 1999) in Santander, Spain.

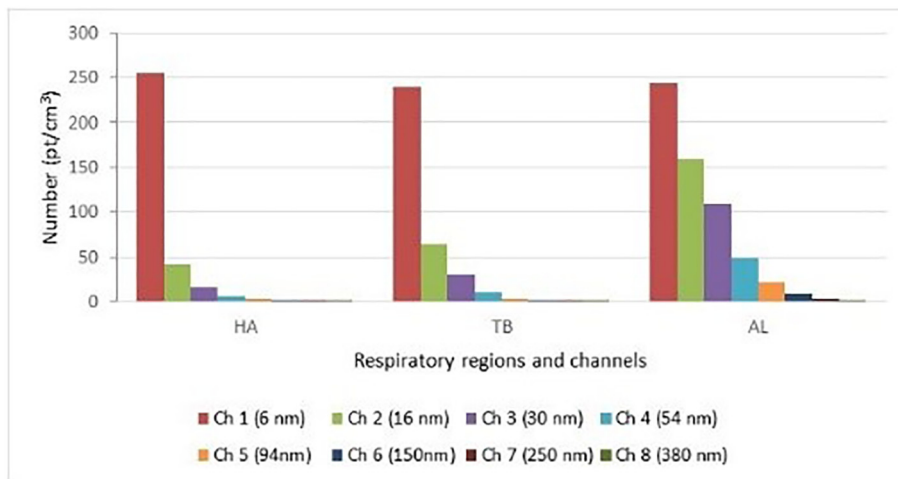


Fig. 2. Deposited nanoparticles by respiratory region and size.

time, when the particles increase their size, there is a higher reduction of nanoparticle deposition at HA and TB than at AL region.

The local deposition fractions proved that the nasal cavity plays a significant role in filtering primary nanoparticles (Löndahl et al., 2014; Wang and Friedlander, 2007).

### 3.2. Surface area

An estimation of the deposited nanoparticles surface area ( $\mu\text{m}^2/\text{cm}^3$ ) has been calculated from the measurements and deposition fraction values corresponding to the whole HRTM (Fig. 3). The outcome of this approach has been called HRT-DSA (deposited surface area).

Surface area for the first two channels is very low ( $\pm 10\%$ ) increasing up to 85% for Ch. 6 (150 nm) and then sharply decreases. The highest values can be found between Ch. 4 (54 nm) and Ch. 8 (380 nm). After applying the HRTM deposition fraction percentage, the distribution of HRT-DSA practically remains unchanged from 6 nm to 150 nm.

Below 150 nm (Ch 6) there are similar values of HRT-DSA due to the deposition fraction (DF) percentages. Surface area measurements show that two groups can be identified. On one hand, from Ch. 1 (6 nm) to Ch. 3 (30 nm) there are high percentages of DF with a plateau HRT-DSA that remain in the three following channels. On the other hand, from Ch. 4

(54 nm) to Ch. 6 (150 nm) there are higher values of surface area but lower percentage of DF.

### 3.3. Surface area by respiratory regions

Fig. 4 shows the DSA by respiratory regions and particle size. Ch. 1 (6 nm) presents the most regular distribution of values of deposited surface area (DSA) per region with about  $60 \mu\text{m}^2/\text{cm}^3$  in each zone. It is also mentionable how relevant the DSA is in the AL, from Ch. 3 (30 nm) to Ch. 6 (150 nm), ( $130$  to  $145 \mu\text{m}^2/\text{cm}^3$ ), compared to the TB and HA regions, except for the first two channels.

There is a progressive slight increase in the TB surface area when the particle area reaches the low range of nanometric scale. In this region, DSA seems to be relevant from Ch. 6 (150 nm) to Ch. 1 (6 nm) when all the channels are studied. As regards HA, apart from Ch. 1 (6 nm), it has low regular deposition along Ch. 2 (16 nm) to Ch. 8 (380 nm). DSA values are similar throughout channels (around  $20 \mu\text{m}^2/\text{cm}^3$ ) except for Ch.1 (6 nm) that registered the highest value over  $60 \mu\text{m}^2/\text{cm}^3$ .

In normal conditions of breathing, small particles (1 nm) will deposit in the upper airways and particles with sizes of 10 nm and 100 nm will end in the airways of the central and peripheral lung. It must be considered that

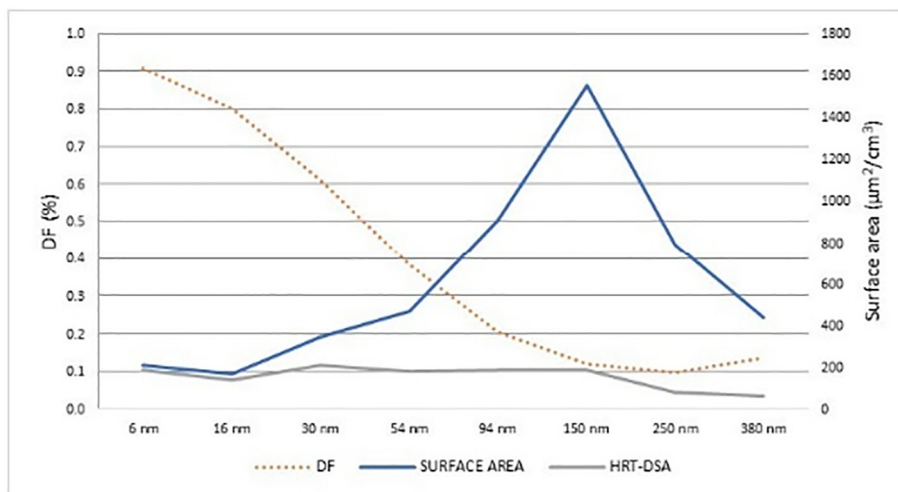


Fig. 3. Total Surface area by size, Deposition Fraction (DF) and HRT-DSA values.

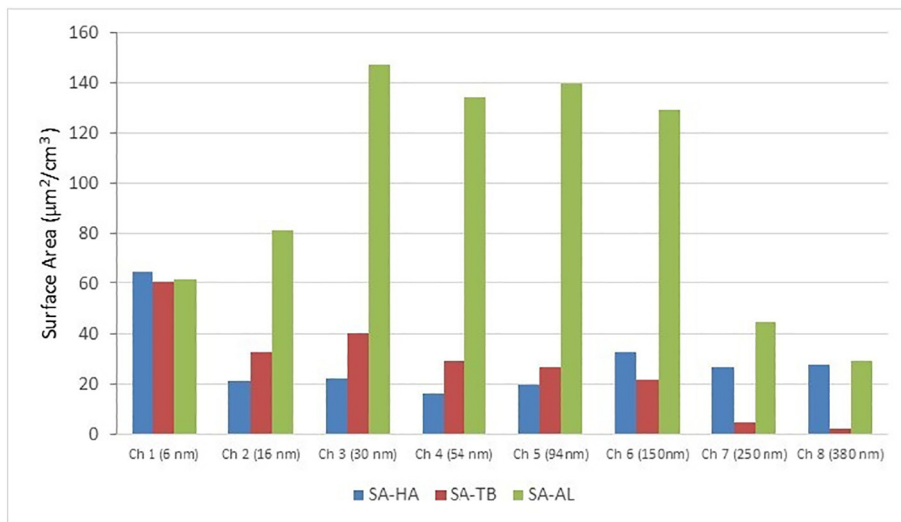


Fig. 4. Deposited surface area by respiratory region and size.

lung morphometry and breathing conditions play a key role in the process of deposition of ultrafine particles (Sturm, 2016).

### 3.4. Electric charge

Fig. 5 shows the sign and magnitude of atmospheric nanoparticles charge measurements for channels 1 to 8 from 4th to 30th July 2018. The data is of hourly average values.

In the subgroup formed by Channel 1 to 4 (6–54 nm), charge takes positive and negative values with extremes from  $-0.70$  f. to  $0.5$  fC. Ch. 2 registered the highest variation coefficient in this subgroup. Ch. 1 seems to be the most stable on measurements which are mainly negative values. Predominance of records with negative charge in Ch 1 (6 nm) and Ch 2 (16 nm) is clear with 86.40% and 58.19% respectively. Records with negative charge decrease to 24.79% when Ch.3 (30 nm) is considered and to 14% for Ch. 4 (54 nm).

In a second subgroup formed by for Ch. 5 (94 nm) to Ch. 8 (380 nm) charge values are always positive. They are inside the threshold from 0.2

to 2 fC. When Ch. 9 (600 nm) is considered, charge varies from  $-3$  f. to 4 fC, registering again negative values.

Negative charge percentages of the low nanoparticles range (Ch. 1 to Ch. 4) is indirectly correlated with particle size. A new hypothesis is emerging as to the role the charge may have in the Brownian deposition mechanisms that characterize the smallest nanoparticles. Knowing how the charge changes from Ch. 1/Ch. 2 to Ch. 3/Ch. 4 could help to explain the role of charge. In this sense, electric charge could also play a key role in the nanoparticles deposition in the respiratory tract which has not been demonstrated yet.

Ch. 1 represent the smallest nanoparticles size measured in this pilot experience and Ch. 2 has the highest alveolar deposition percentage which might be associated to the wellbeing generated by negative ions atmospheric environments. The geographic location where the measurements were conducted may influence, to some extent, the presence of high percentages of negative charge in the smallest nanoparticles. It is perhaps linked to maritime aerosol being ionized in salty air masses.

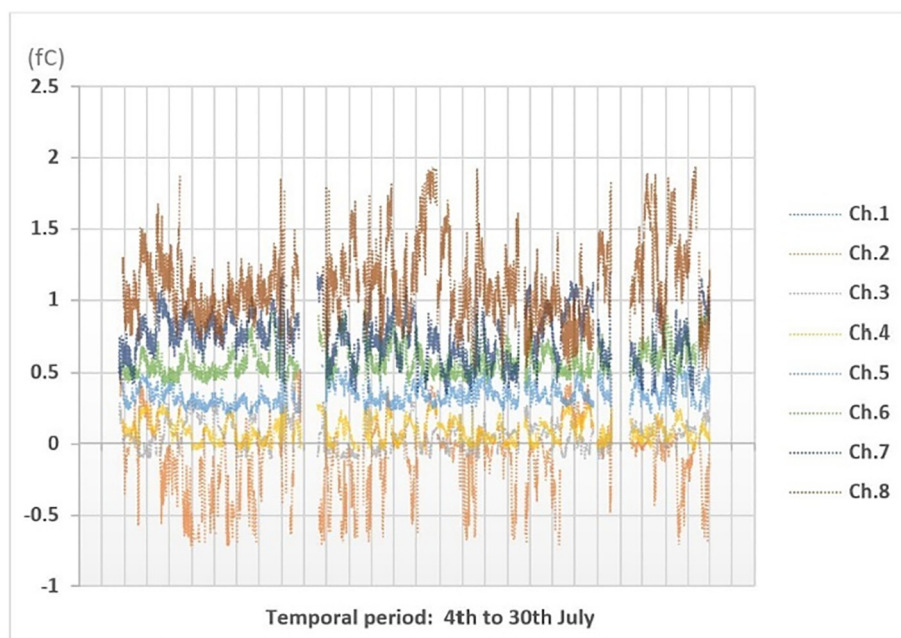


Fig. 5. Nanoparticles electric charge from Ch.1 to Ch. 8 (range 6 nm–380 nm).

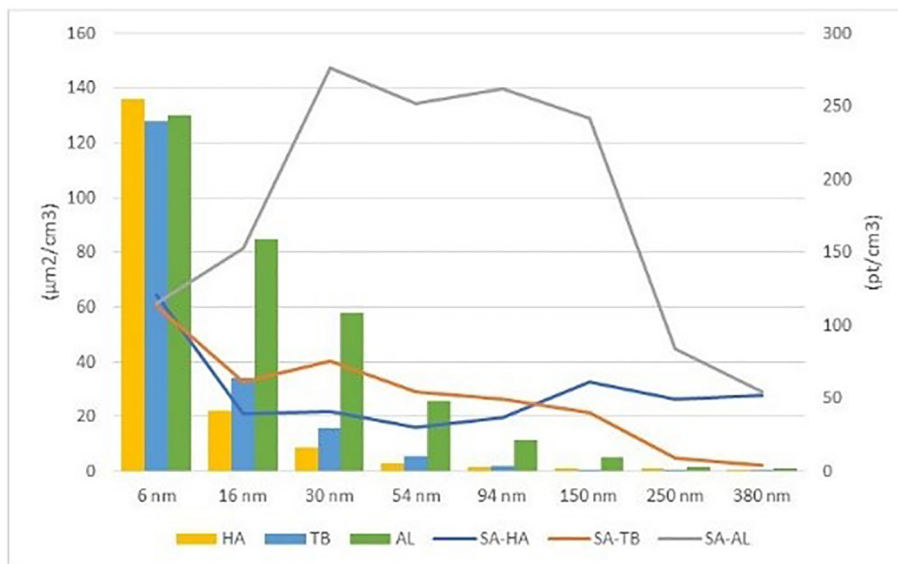


Fig. 6. Surface area and number by particle size and respiratory regions.

Nanoparticles smaller than 6 nm can deposit easily at HA. They can translocate to the brain through the olfactory and trigeminal nerves. Negative charge can facilitate deposition in the brain. At the same time, the presence of primary nanoparticles in the brain area can have negative impacts on health.

Fig. 6 compares surface area and number by particle size through respiratory regions. Number shows a gradual reduction from Ch. 1 to Ch. 8. This figure presents primary and secondary nanoparticles in the three HRT regions. Deposited surface area in alveolar region presents a very different distribution by nanoparticle size compared to the other two respiratory regions. It presents a plateau with high values from Ch. 3 to Ch. 6 where reach an average of 140 µm²/cm³.

Overall, number for AL region is just decreasing by channel and coincides with Brownian deposited mechanism behavior. The AL region holds a significant number of nanoparticles from 16 nm–150 nm comparing to TB and HA regions. The number for HA sharply decreases from Ch.1 to Ch.2 and for TB zone but less sharply. These findings

indicate that the TB area deposits more nanoparticles than HA at 16 nm–94 nm.

This result allows us to point out the singular behavior of the DSA as a nanoparticle unit measurement, different from the number when studying its role in the field of nanotoxicity. The increase in the surface area of the nanoparticles in the alveolar area matches with a change in the polarity (electrical charge) of the nanoparticles from negative to positive from 16 nm to 30 nm.

### 3.5. Sample characterization

Samples taken from the selected channels were characterized with Transmission Electronic Microscopy (Jeol Jem 2100 with XEDS) and Raman Spectroscopy (T 64000, Horiba-Jobin-Yvon).

TEM showed a mainly spherical morphology. Elemental analysis revealed carbon (C) (Fig. 7) partially formed by multiwalled carbon nanotubes and the presence of silica (SiO2) and iron oxides (Fig. 8).

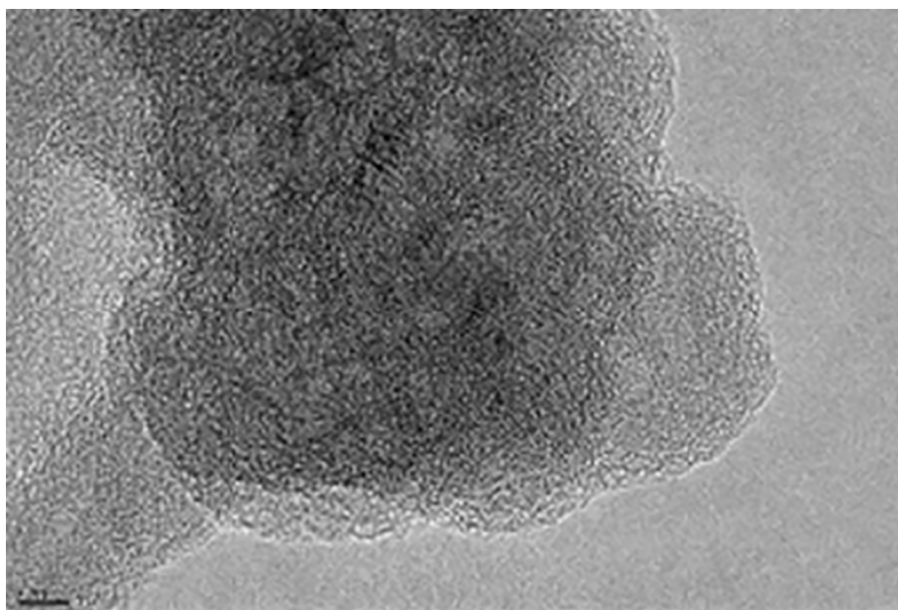


Fig. 7. Carbon partially formed by multiwalled carbon nanotubes. 5 nm TEM morphology study.

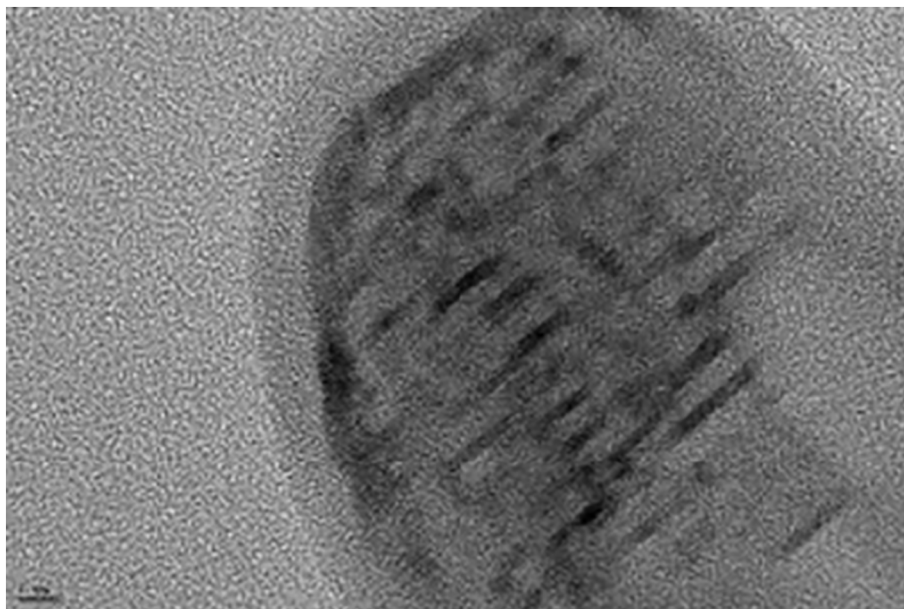


Fig. 8. Iron oxides with their rectangular internal structure. TEM morphology study.

Raman detected the presence of disordered graphite. Graphite pentagonal defects let the formation of multiwalled carbon nanotubes, giving flexibility and allowing them to bend (Fig. 7). It was also determined the presence of iron oxide nanoparticles in samples (hematite  $\alpha$   $\text{Fe}_2\text{O}_3$ , Lepidocrocite  $\gamma$  and  $\delta$   $\text{FeOOH}$  and Siderite  $\text{FeCO}_3$ ) (Fig. 8). The OH vibration of lepidocrocite comes from the presence of water vapor.

#### 4. Conclusions

Atmospheric nanoparticles showed a higher number at 6 nm–16 nm. Negative charge of nanoparticles is clearly associated to the smallest channels where Brownian deposition is predominant. In this sense, electric charge becomes a determining factor in the Brownian behavior of atmospheric nanoparticles (6 nm–150 nm) what may have relevant implications for human health.

Change in polarity leads to a significant increase in alveolar deposition in terms of surface area, switching from 16 nm to 30 nm. Transition from primary to secondary nanoparticles is consistent with a decrease on number and positive charge values.

The results show the importance of taking measurements of atmospheric particulate matter below the legal sizes to better understand the links between atmospheric pollutants and human health. Nanoparticle electric charge must also be considered in these new measurements. The toxicological effects of the samples collected, mainly in those cases in which the alveolar surface area has a greater deposition, remain to be studied.

The length of the time series recorded is a limitation nowadays for the development of an electrical classification of weather types based on particles electrical properties, which is a future study. Further continuous collection of data is also needed to confirm conclusions mentioned in this work. Future work should aim to confirm that nanoparticle electrical charge is dependent on size in different environments and geographic locations.

#### CRedit authorship contribution statement

Pablo Fdez-Arroyabe: Conceptualization, Research plan, Supervision. Ciro Salcines: Original draft preparation, Data curation, Visualization, Formal analysis, Investigation, Writing. Pavlo Kassomenos: Investigation, Reviewing. Ana Santurtún: Conceptualization, Original draft preparation. Tuukka Petäjä: Reviewing.

#### Declaration of competing interest

The authors declare that they have no known competing financial interest or personal relationship that could have appeared to influence the work reported in this paper.

#### Acknowledgements

The authors would like to acknowledge Dekati Ltd. and SOLMA Environmental Solutions for providing instrument to the study and Dr. Amelia Cummins for her wise counsel. Partial financial support was provided through COST-Action 15211 and from the Spanish National Research Agency: Project B487 (CSO2016.75154-R) Title: Healthy cities: acute respiratory diseases in Spain and biometeorological alerts. We would like to thank (alphabetic order) to Dr. Israel Cano-Rico, Prof. Dr. Reik Doner, Dr. Andrei Niță and Prof. Rafael Valiente for their support in specific aspects related to sample preparation, data management and interpretation in specific moments of this research.

#### References

- Brown, D.M., Wilson, M.R., MacNee, W., Stone, V., Donaldson, K., 2001. Size-dependent pro-inflammatory effects of ultrafine polystyrene particles: a role for surface area and oxidative stress in the enhanced activity of ultrafines. *Toxicol. Appl. Pharmacol.* 175, 191–199. <https://doi.org/10.1006/taap.2001.9240>.
- Campbell, P., Zhang, Y., Yan, F., Lu, Z., Streets, D., 2018. Impacts of transportation sector emissions on future U.S. air quality in a changing climate. Part II: Air quality projections and the interplay between emissions and climate change. *Environ. Pollut.* 238, 918–930. <https://doi.org/10.1016/j.envpol.2018.03.016>.
- Chu, C.H., Chen, S.R., Wu, C.H., Cheng, Y.C., Cho, Y.M., Chang, Y.K., 2019. The effects of negative air ions on cognitive function: an event-related potential (ERP) study. *Int. J. Biometeorol.* 63, 1309–1317. <https://doi.org/10.1007/s00484-019-01745-7>.
- Commission, E., 2011. *EC Nanomaterial Definition 2010–2012*.
- Dekati, 2018. *ELPI+ Manual*.
- Deng, Q., Ou, C., Chen, J., Xiang, Y., 2018. Particle deposition in tracheobronchial airways of an infant, child and adult. *Sci. Total Environ.* 612, 339–346. <https://doi.org/10.1016/j.scitotenv.2017.08.240>.
- Deng, Q., Deng, L., Miao, Y., Guo, X., Li, Y., 2019. Particle deposition in the human lung: Health implications of particulate matter from different sources. *Environ. Res.* 169, 237–245. <https://doi.org/10.1016/j.envres.2018.11.014>.
- Donaldson, K., Tran, C.L., 2002. Inflammation caused by particles and fibers. *Inhal. Toxicol.* 14, 5–27. <https://doi.org/10.1080/089583701753338613>.
- Donaldson, K., Li, X.Y., MacNee, W., 1998. Ultrafine (nanometre) particle mediated lung injury. *J. Aerosol Sci.* 29, 553–560. [https://doi.org/10.1016/S0021-8502\(97\)00464-3](https://doi.org/10.1016/S0021-8502(97)00464-3).
- Donaldson, K., Tran, L., Jimenez, L.A., Duffin, R., Newby, D.E., Mills, N., MacNee, W., Stone, V., 2005. Combustion-derived nanoparticles: a review of their toxicology following inhalation exposure. Part. *Fibre Toxicol.* 2. <https://doi.org/10.1186/1743-8977-2-10>.

- Fdez-Arroyabe, P., Salcines Suárez, C.L., Nita, I.A., Kassomenos, P., Petrou, E., Santurtún, A., 2020. Electrical characterization of circulation weather types in northern Spain based on atmospheric nanoparticles measurements: a pilot study. *Sci. Total Environ.* 704, 135320. <https://doi.org/10.1016/j.scitotenv.2019.135320>.
- Fisher, B., 2002. Meteorological factors influencing the occurrence of air pollution episodes involving chimney plumes. *Meteorol. Appl.* 9, 199–210. <https://doi.org/10.1017/S1350482702002050>.
- Geiser, M., Kreyling, W.G., 2010. Deposition and biokinetics of inhaled nanoparticles. *Part. Fibre Toxicol.* 7, 2. <https://doi.org/10.1186/1743-8977-7-2>.
- Ghorani-Azam, A., Riahi-Zanjani, B., Balali-Mood, M., 2016. Effects of air pollution on human health and practical measures for prevention in Iran. *J. Res. Med. Sci.* <https://doi.org/10.4103/1735-1995.189646>.
- Hamana, R.B., Mutlu, G.M., 2018. Particulate matter air pollution: effects on the cardiovascular system. *Front. Endocrinol. (Lausanne)*, 9 <https://doi.org/10.3389/fendo.2018.00680>.
- Hawkins, L.H., 1981. The influence of air ions, temperature and humidity on subjective wellbeing and comfort. *J. Environ. Psychol.* 1, 279–292. [https://doi.org/10.1016/S0272-4944\(81\)80026-6](https://doi.org/10.1016/S0272-4944(81)80026-6).
- Health Organization, W., Organization, W., Office for Europe, R., 2013. *Health Effects of Particulate Matter*.
- Held, A., Zerrath, A., McKeon, U., Fehrenbach, T., Niessner, R., Plass-Dülmer, C., Kaminski, U., Berresheim, H., Pöschl, U., 2008. Aerosol size distributions measured in urban, rural and high-alpine air with an electrical low pressure impactor (ELPI). *Atmos. Environ.* 42, 8502–8512. <https://doi.org/10.1016/j.atmosenv.2008.06.015>.
- Hinds, W.C., 1999. *Aerosol technology: properties, behaviour, and measurement of airborne particles*. Respiratory Deposition, Second. ed Wiley-Interscience, New York.
- ICRP, 1994. *Human Respiratory Tract Model for Radiological Protection*, Annual. 66. ed. .
- Inbar, O., Rotstein, A., Dlin, R., Dotan, R., Sulman, F.G., 1982. The effects of negative air ions on various physiological functions during work in a hot environment. *Int. J. Biometeorol.* 26, 153–163. <https://doi.org/10.1007/BF02184628>.
- International Commission on Radiological Protection, 1994. *Human Respiratory Tract Model for Radiological Protection*, Annual. 66. ed. .
- Järvinen, A., Aitoma, M., Rostedt, A., Keskinen, J., Yli-Ojanperä, J., 2014. Calibration of the new electrical low pressure impactor (ELPI+). *J. Aerosol Sci.* 69, 150–159. <https://doi.org/10.1016/j.jaerosci.2013.12.006>.
- Järvinen, A., Heikkilä, P., Keskinen, J., Yli-Ojanperä, J., 2017. Particle charge-size distribution measurement using a differential mobility analyzer and an electrical low pressure impactor. *Aerosol Sci. Technol.* 51, 20–29. <https://doi.org/10.1080/02786826.2016.1256469>.
- Kottek, M., Grieser, J., Beck, C., Rudolf, B., Rubel, F., 2006. World map of the Köppen-Geiger climate classification updated. *Meteorol. Z.* 15, 259–263. <https://doi.org/10.1127/0941-2948/2006/0130>.
- Krueger, A.P., Reed, E.J., 1976. Biological impact of small air ions. *Science* 193, 1209–1213. <https://doi.org/10.1126/science.959834>.
- Lappalainen, H., Petäjä, T., Vihma, T., Räisänen, J., Baklanov, A., Chalov, S., Esau, I., Ezhova, E., Leppäranta, M., Pozdnyakov, D., Pumpunanen, J., Andreae, M., Arshinov, M., Asmi, E., Bai, J., Bashmachnikov, I., Belan, B., Bianchi, F., Biskaborn, B., Boy, M., Bäck, J., Cheng, B., Chubarova, N.Y., Duplissy, J., Dyukarev, E., Eleftheriadis, K., Forsius, M., Heimann, M., Juhola, S., Kononov, V., Kononov, I., Konstantinov, P., Koster, K., Lapsina, E., Lintunen, A., Mahura, A., Makkonen, R., Malkhazova, S., Mammarella, I., Mammola, S., Mazon, S., Meinander, O., Mikhailov, E., Miles, V., Myselko, S., Orlov, D., Paris, J.-D., Pirazzini, R., Popovicheva, O., Pulliainen, J., Rautiainen, K., Sacks, T., Shevchenko, V., Skorokhod, A., Stohl, A., Suhonen, E., Thomson, E., Tsidilina, M., Tynkynen, V.-P., Uotila, P., Virkkula, A., Voropay, N., Wolf, T., Yasunaka, S., Zhang, J., Qiu, Y., Ding, A., Guo, H., Bondur, V., Kasimov, N., Zilitinkevich, S., Kerminen, V.-M., Kulmala, M., 2021. Overview: recent advances on the understanding of the Northern Eurasian environments and of the urban air quality in China - Pan Eurasian Experiment (PEEX) program perspective. *Atmos. Chem. Phys.*, 1–106 <https://doi.org/10.5194/ACP-2021-341>.
- Lepistö, T., Kuuluvainen, H., Juuti, P., Järvinen, A., Arffman, A., Rönkkö, T., 2020. Measurement of the human respiratory tract deposited surface area of particles with an electrical low pressure impactor. *Aerosol Sci. Technol.* 54, 958–971. <https://doi.org/10.1080/02786826.2020.1745141>.
- Liu, W., Huang, J., Lin, Y., Cai, C., Zhao, Y., Teng, Y., Mo, J., Xue, L., Liu, L., Xu, W., Guo, X., Zhang, Y., Zhang, J., 2021. Negative ions offset cardiorespiratory benefits of PM<sub>2.5</sub> reduction from residential use of negative ion air purifiers. *Indoor Air* 31, 220–228. <https://doi.org/10.1111/ina.12728>.
- Löndahl, J., Möller, W., Pagels, J.H., Kreyling, W.G., Swietlicki, E., Schmid, O., 2014. Measurement techniques for respiratory tract deposition of airborne nanoparticles: a critical review. *J. Aerosol Med. Pulm. Drug Deliv.* 27, 229–254. <https://doi.org/10.1089/jamp.2013.1044>.
- Maczyński, B., Tyczka, S., Marecki, B., Góra, T., 1971. Effect of the presence of man on the air ion density in an office room. *Int. J. Biometeorol.* 15, 11–21. <https://doi.org/10.1007/BF01804715>.
- Manisalidis, I., Stavropoulou, E., Stavropoulos, A., Bezirtzoglou, E., 2020. Environmental and health impacts of air pollution: a review. *Front. Public Health* <https://doi.org/10.3389/fpubh.2020.00014>.
- Marjamäki, M., Keskinen, J., Chen, D.-R., Pui, D.Y.H., 2000. Performance evaluation of the electrical low-pressure impactor (ELPI). *J. Aerosol Sci.* 31, 249–261.
- Oberdörster, G., 2000. Toxicology of ultrafine particles: in vivo studies. *Philos. Trans. R. Soc. A Math. Phys. Eng. Sci.* 358, 2719–2740.
- Oberdörster, G., Yu, C.P., 1990. The carcinogenic potential of inhaled diesel exhaust: a particle effect? *J. Aerosol Sci.* 21, S397–S401. [https://doi.org/10.1016/0021-8502\(90\)90265-Y](https://doi.org/10.1016/0021-8502(90)90265-Y).
- Oberdörster, G., Ferin, J., Gelein, R., Soderholm, S.C., Finkelstein, J., 1992. Role of the alveolar macrophage in lung injury: studies with ultrafine particles. *Environ. Health Perspect.* 97, 193–199. <https://doi.org/10.1289/ehp.97-1519541>.
- Oberdörster, G., Maynard, A., Donaldson, K., Castranova, V., Fitzpatrick, J., Ausman, K., Carter, J., Kam, B., Kreyling, W., Lai, D., Warheit, D., Yang, H., 2005a. Principles for characterizing the potential human health effects from exposure to nanomaterials: elements of a screening strategy. *Part. Fibre Toxicol.* 2. <https://doi.org/10.1186/1743-8977-2-8>.
- Oberdörster, G., Oberdörster, E., Oberdörster, J., 2005b. Nanotoxicology: an emerging discipline evolving from studies of ultrafine particles. *Environ. Health Perspect.* <https://doi.org/10.1289/ehp.7339>.
- Oberdörster, G., Elder, A., Rinderknecht, A., 2009. Nanoparticles and the brain: cause for concern? *J. Nanosci. Nanotechnol.* 9, 4996–5007. <https://doi.org/10.1166/jnn.2009.gr02>.
- Peters, A., Wichmann, H.E., Tuch, T., Heinrich, J., Heyder, J., 1997. Respiratory effects are associated with the number of ultrafine particles. *Am. J. Respir. Crit. Care Med.* 155, 1376–1383. <https://doi.org/10.1164/ajrccm.155.4.9105082>.
- Qiao, H., Liu, W., Gu, H., Wang, D., Wang, Y., 2015. The transport and deposition of nanoparticles in respiratory system by inhalation. *J. Nanomater.* <https://doi.org/10.1155/2015/394507>.
- Rothen-Rutishauser, B., Blank, F., Mühlfeld, C., Gehr, P., 2008. In vitro models of the human epithelial airway barrier to study the toxic potential of particulate matter. *Expert Opin. Drug Metab. Toxicol.* 4. <https://doi.org/10.1517/17425255.4.8.1075>.
- Santurtún, H., Liu, W., Gu, H., Wang, D., Wang, Y., 2015. The transport and deposition of nanoparticles in respiratory system by inhalation. *J. Nanomater.* <https://doi.org/10.1155/2015/394507>.
- Santurtún, A., Rasilla, D.F., Riancho, L., Zarrabaitia, M.T., 2017. Relationship between chronic obstructive pulmonary disease and air pollutants depending on the origin and trajectory of air masses in the north of Spain. *Arch. Bronconeumol.* 53, 616–621. <https://doi.org/10.1016/j.arbres.2017.03.017>.
- Schraufnagel, D.E., 2020. The health effects of ultrafine particles. *Exp. Mol. Med.* <https://doi.org/10.1038/s12276-020-0403-3>.
- Shenfeld, L., 2011. To cite this article: L. Shenfeld (1970) meteorological aspects of air pollution control. *Atmosphere (Basel)* 8, 3–13. <https://doi.org/10.1080/00046973.1970.9676578>.
- Shindell, D., Smith, C.J., 2019. Climate and air-quality benefits of a realistic phase-out of fossil fuels. *Nature* 573, 408–411. <https://doi.org/10.1038/S41586-019-1554-Z>.
- Sturm, R., 2016. Local lung deposition of ultrafine particles in healthy adults: experimental results and theoretical predictions. *Ann. Transl. Med.* 4. <https://doi.org/10.21037/atm.2016.11.13> 4-4.
- Tran, C.L., 2000. Inhalation of poorly soluble particles. II. Influence of particle surface area on inflammation and clearance. *Inhal. Toxicol.* 12, 1113–1126. <https://doi.org/10.1080/08958370050166796>.
- Tran, C.L., Cullen, R.T., Jones, A.D., Donaldson, K., 1998. Influence of particle characteristics on the clearance of low toxicity dust from lungs. *J. Aerosol Sci.* 29, 1269–1270.
- Wang, C., Friedlander, S.K., 2007. Determination of surface area and volume of nanoparticle aggregates deposited in the human respiratory tract using DMA data. *J. Aerosol Sci.* 38, 980–987. <https://doi.org/10.1016/j.jaerosci.2007.07.002>.
- Wichmann, H.E., Spix, C., Tuch, T., Wölke, G., Peters, A., Heinrich, J., Kreyling, W.G., Heyder, J., 2000. Daily mortality and fine and ultrafine particles in Erfurt, Germany part I: role of particle number and particle mass. *Res. Rep. Health. Eff. Inst.* 98, 5–86 discussion 87–94. PMID: 11918089.
- Yang, L., Li, C., Tang, X., 2020. The impact of PM<sub>2.5</sub> on the host defense of respiratory system. *Front. Cell Dev. Biol.* <https://doi.org/10.3389/fcell.2020.00091>.
- Zhang, H., Xu, T., Zong, Y., Tang, H., Liu, X., Wang, Y., 2015. Influence of meteorological conditions on pollutant dispersion in street canyon. *Procedia Eng.* 121, 899–905. <https://doi.org/10.1016/J.PROENG.2015.09.047>.